

USING THE RESPONSE SURFACE METHODOLOGY (RSM) TO IMPROVE THE CUTTING OF S355J2C+N STEEL

Aneta JAKUBUS^{*}, Joanna KOSTRZEWA^{*}, Marcin JASIŃSKI^{*}, Bartłomiej Wik^{*}, Maciej NADOLSKI^{**}

^{*}Technical Department, The Jacob of Paradies University in Gorzów Wielkopolski ul. Teatralna 25, 66-400 Gorzów Wielkopolski, Poland

^{**}Faculty of Production Engineering and Materials Technology, Częstochowa University of Technology, Al. Armii Krajowej 19, 42-201 Częstochowa, Poland

jakubusaneta@wp.pl, jkostrzewska@wp.pl, mjasinski@ajp.edu.pl, bartek.wik11@gmail.com, nadolski.maciej@wip.pcz.pl

received 09 March 2025, revised 07 October 2025, accepted 07 October 2025

Abstract: This article presents research on the evaluation of the influence of various fiber laser parameters on the quality of the surface after the cutting process. The study was conducted using a 10 mm thick S355J2C+N steel sheet. The cutting process was performed on a Fiber Laser VF1530 cutting machine with a power of 4000 W, manufactured by Otinus. To develop a model of the laser cutting process, the response surface methodology (RSM) was applied. A second-degree polynomial equation was selected to construct the model. The study found that the parameter R_c exhibited a predicted coefficient of determination of 99.89% for the variance of laser settings in steel cutting, in relation to the roughness of the upper part of the intersection surface. The results demonstrated that the value of R_c is significantly influenced by cutting speed, the interaction between speed and peak power, the interaction between focus and speed, as well as the peak power parameter. Surface topography analysis revealed that as the laser beam power increased in relation to the cross-cutting speed, additional material melting occurred, leading to an increase in surface roughness. However, when the cross-cutting speed was increased while maintaining constant power, surface roughness decreased.

Key words: laser cutting, response surface methodology (RSM), process optimization, structural steel

1. INTRODUCTION

Laser cutting is one of the most commonly used thermal cutting methods. This technology utilizes a concentrated beam of photons, enabling precise cutting of complex steel and other materials while maintaining high accuracy and quality of cut surfaces, with a narrow heat-affected zone (HAZ) [1–6]. The quality of the cutting surface is influenced by multiple factors, including the type of material being cut, selected cutting parameters (e.g., laser beam power, assist gas, feed rate, lens type, and focal length), as well as the correct setup and operation of the laser cutting system [1–10]. To assess the appropriateness of laser or plasma cutting parameters for different materials, previous studies have primarily focused on evaluating lateral surface perpendicularity, cut surface roughness, kerf width, and the heat-affected zone [1–10]. In some cases, the obtained results have been compared with relevant industry standards [11].

In the study presented in [2], roughness parameters R_a , R_z , R_t , R_p , and R_v were measured on both the laser-exposed and opposite sides of the material to compare the cutting surfaces of selected structural materials processed using plasma and laser cutting. Additionally, microstructural analysis was conducted. The comparative results demonstrated a significant advantage of laser cutting over plasma cutting.

Similarly, research described in [7] used the roughness parameter R_{z5} to analyze the surfaces of S355J2 steel cut by plasma, alongside hardness (HV10) measurements and perpendicularity assessments. The study concluded that the skill and experience of

the operator had a substantial impact on the quality of plasma-cut edges. Preliminary findings obtained through 3D scanning indicated that cutting parameters should not solely rely on the manufacturer's recommended settings. Furthermore, Daniel J. Thomas [12] investigated the stability of laser-cut edges in high-stress locations on structural beams, concluding that surface roughness characteristics could serve as indicators of fatigue life.

To develop models and optimize the laser cutting process, the Design of Experiments (DoE) methodology can be employed. This approach allows for the extraction of a large amount of data from a limited number of experiments, reducing the number of required tests and overall processing time. Tests can be conducted using a full factorial design, and response surface methodology (RSM)—a combination of mathematical and statistical modeling—can be applied for multi-criteria optimization. Many researchers have used this method to analyze and optimize cutting processes [13–15]. For example, in [16], RSM was employed to model the abrasive water-jet cutting (AWSJ) process of a composite material (phenolic resin reinforced with cotton fabric), identifying optimal control parameters to enhance cutting depth efficiency. In another study [17], RSM was used to assess the influence of key process parameters on the accuracy and surface quality of plasma arc cutting (PAC) for Monel 400 steel.

This study explores the optimization of the laser cutting process for S355J2C+N steel, with particular emphasis on improving cut surface quality and accuracy using response surface methodology (RSM). There is a limited number of studies addressing this specific topic. The upper zone of the cut surface was analyzed due to the

presence of irregularities in the form of striations.

These surface fringes are a major determinant of edge roughness in laser cutting and serve as key quality indicators. Their formation is influenced by both laser cutting parameters and the material properties of the workpiece [12, 18, 19]. The primary objective of this study is to minimize height variations in the surface profile, which can contribute to stress concentration and crack initiation, thereby enhancing the structural integrity of laser-cut components.

2. RESEARCH METHODOLOGY

The experiments were conducted on hot-rolled S355J2C+N non-alloy structural steel, supplied in the form of sheet metal after normalization [20]. The chemical composition and minimum mechanical properties of the tested material are presented in Table 1.

Tab. 1. Chemical composition and minimum mechanical properties of S355J2C+N steel [20]

Maximum element content, %					
C	Mn	Si	P	S	N
0.22	1.5	0.55	0.035	0.035	-
Minimal mechanical properties					
ReH MPa	Rm MPa		A %		
355	490		20		

The experimental studies aimed to evaluate the influence of various fiber laser parameters on the surface morphology after the cutting process. The tests were conducted on a 10 mm thick sheet of S355J2C+N steel, using a Fiber Laser VF1530 cutting machine with a power of 4000 W (manufactured by Otinus). A double nozzle with a 1.2 mm diameter was used for cutting, and oxygen was selected as the processing gas at a pressure of 0.9 bar. For analysis, samples measuring 52.5 × 25 × 10 mm were cut from the sheet [21].

The cut surface was examined using an Olympus DSX 1000 digital microscope (Olympus Corp., Tokyo, Japan). Surface roughness analysis was performed at three locations in the upper part of the cut surface, measured from the top of the sample at distances of 750 µm, 1000 µm, and 1250 µm. The measurements were conducted using Lext software, specifically designed for the Olympus DSX 1000 microscope. The cut surface was also observed using the Axia ChemisSEM Scanning Electron Microscope from ThermoFisher Scientific. The images were captured from the analyzed upper section of the cut surface at magnifications of 200x and 2000x.

For the roughness analysis, the amplitude parameter R_c was used. R_c , known as the mean height of profile elements, represents the average height variation of surface features over the sampling length. It provides a measure of the central tendency of surface roughness peaks and valleys, offering insight into the overall surface texture. R_c is particularly valuable for surface characterization where a uniform distribution of peaks and valleys is crucial. While many studies focus on R_z (maximum height) and R_a (arithmetic mean deviation) parameters [22–25], R_c was selected for this study as it accounts for the average height of individual profile elements

rather than just extreme values (R_z) or absolute mean deviations (R_a). Additionally, R_c is less sensitive to single extreme values, as it considers a greater number of measurement points compared to R_z .

The steel cutting process was conducted based on factorial experimental design. Statistical data analysis was performed using Minitab 21.1 software (Pennsylvania State University, Pennsylvania, PA, USA). A comprehensive factorial plan was applied to determine the effects of focal length (mm), feed rate (mm/s), and peak power (W) on surface roughness (R_c). The main effects and bidirectional interactions were analyzed using a mathematical model describing the relationships between variables. The function defining these relationships typically takes the form of second-degree polynomials, expressed as:

$$\hat{y} = b_0 + \sum_{i=1}^n b_i x_i + \sum_{1 \leq x \neq j} b_{ij} (x_i x_j) \quad (1)$$

where in the formula the calculated value of the parameter is marked as \hat{y} , b_0 – intercept, b_i regression coefficients of the linear terms of the model, x_i – linear terms of the factors, b_{ij} regression coefficients of the terms of the double coefficients, $x_i x_j$ – terms of the interaction of the double factors x_i and x_j .

The tests were conducted based on three independent variables, namely focal length, feed rate, and peak power. The following designations and parameter ranges were adopted:

- X_1 – focal length: 0.2 mm to 0.3 mm,
- X_2 – feed speed: 25.334 mm/s to 28.000 mm/s,
- X_3 – peak power: 3600 W to 4000 W.

These parameters were selected because the values recommended by the sheet metal manufacturer did not allow for a successful cut. The figure below presents an example of a cutting attempt using the manufacturer's recommended settings. These settings were as follows:

- Focal length: 5 mm,
- Feed speed: 30.833 mm/s,
- Peak power: 4000 W.

With these parameters, it was not possible to achieve a complete cut or to separate the element from the sheet metal.



Fig. 1. An attempt to cut out samples from S355J2C+N steel using the manufacturer's parameters: a) surface view, b) underside view

3. RESULTS AND DISCUSSION

The results of the surface roughness measurements obtained for the given laser operating parameters are presented in Table 2. The table also includes the results calculated using the (\hat{Y}') model. It can be observed that an increase in power, relative to a cross-cutting speed of 25.334 mm/s, resulted in additional melting of the material, leading to greater surface roughness. However, when the cross-cutting speed increased, the surface roughness decreased again.

Figure 2 presents an example of the surface topography, while Figures 3 and 4 display photographs of the side surfaces of the cut samples, including measurement site markings. Laser-cut edges produced using different parameter settings exhibit distinctive surface characteristics. On the lateral surface of the material, zones with different topographic features can be identified (see Fig. 4a). Zone 1: Regular and evenly distributed striations are visible, with an average width of approximately 250 μm , covering about 30% of the assessed area. Zone 2: The striations disappear, and the surface becomes more homogeneous.

Tab. 2. Cutting parameters used

Steel S355J2C+N Laser Settings					
	Focus [mm]	Speed [mm/s]	Peak Power [W]	Mount Rc	
	X ₁	X ₂	X ₃	Y	Y'
1	2	3	4	5	6
1	0.2	25.334	3600	45.82	45.65
2	0.2	25.334	4000	61.56	61.73
3	0.2	28	3600	55.01	55.18
4	0.2	28	4000	43.00	42.84
5	0.3	25.334	3600	58.41	58.58
6	0.3	25.334	4000	79.70	79.53
7	0.3	28	3600	42.88	42.71
8	0.3	28	4000	35.07	35.24

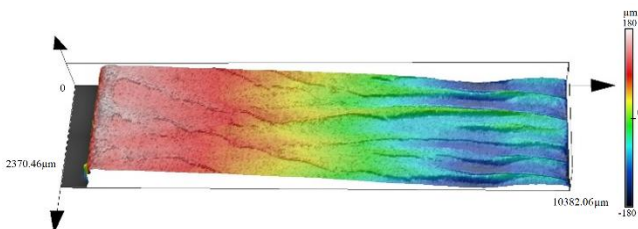


Fig. 2. Example of surface topography obtained at the following settings: focal length 0.2 mm; feed rate 28 mm/s and peak power 3600 W (see Table 1 column 1, sample number 3)

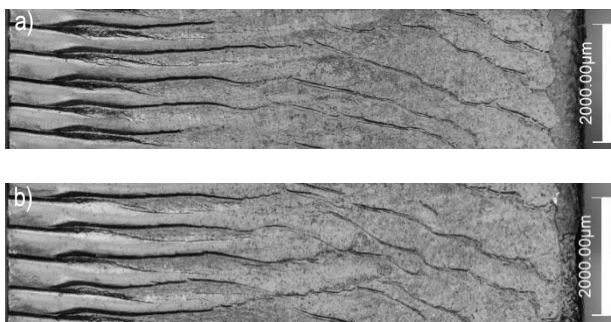


Fig. 3. Photographs of the lateral surface of the cut specimen according to the parameters marked in Table 2, Column 1, as: a) Sample 1, b) Sample 2.

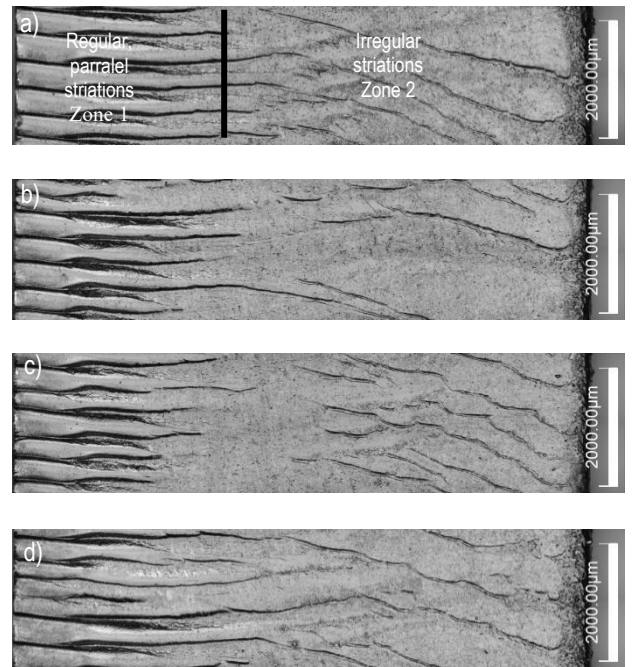


Fig. 4. Photographs of the lateral surface of the cut specimen according to the parameters marked in Table 2, Column 1, as: a) Sample 5, b) Sample 6, c) Sample 7, d) Sample 8

Table 3 presents the overall ANOVA results for main effects and two-factor interactions, analyzed at a 95% confidence level ($\alpha = 0.05$). The main effects, such as feed speed ($p = 0.012$) and peak power ($p = 0.049$), were found to be statistically significant. The interaction between feed rate and peak power, as well as focal length and feed speed, significantly affected surface roughness.

Tab. 3. Analysis of variance (ANOVA) results for the influence of cutting parameters on Rc

Source	DF	Adj SS	Adj MS	F-Value	P-Value
1	2	3	4	5	6
Model	6	1393.79	232.298	1039.10	0.024
Linear	3	655.54	218.513	977.44	0.024
Focal length [mm]	1	14.18	14.176	63.41	0.080
Feed speed [mm/s]	1	604.34	604.337	2703.27	0.012
Peak power [W]	1	37.03	37.026	165.62	0.049
2-Way Interaction	3	738.25	246.083	1100.76	0.022
Focal length [mm]*Feed speed [mm/s]	1	322.51	322.512	1442.64	0.017
Focal length [mm]*Peak power [W]	1	11.87	11.868	53.09	0.087
Feed speed [mm/s]*Peak power [W]	1	403.87	403.867	1806.55	0.015
Error	1	0.22	0.224		
Total	7	1394.01			

*DF- degree of freedom; SS - sum of squares; MS - mean square; F - ratio of variance error

Figure 5 illustrates a Pareto plot of standard-ized effects, obtained from analysis of variance (ANOVA) for main effects and two-factor interactions. Additionally, the figure includes a normal probability plot of residuals and a predicted versus actual plot, which confirm that the model provides a good fit to the experimental data and that the residuals are approximately normally distributed. Although the normal probability plot of residuals indicates a departure from normality ($AD = 1.282$, $p < 0.005$), the predicted-versus-actual plot shows close agreement with the data (points along the 45° line), confirming very good model fit. The graph Pareto indicates that feed rate is the most statistically significant factor affecting surface roughness.

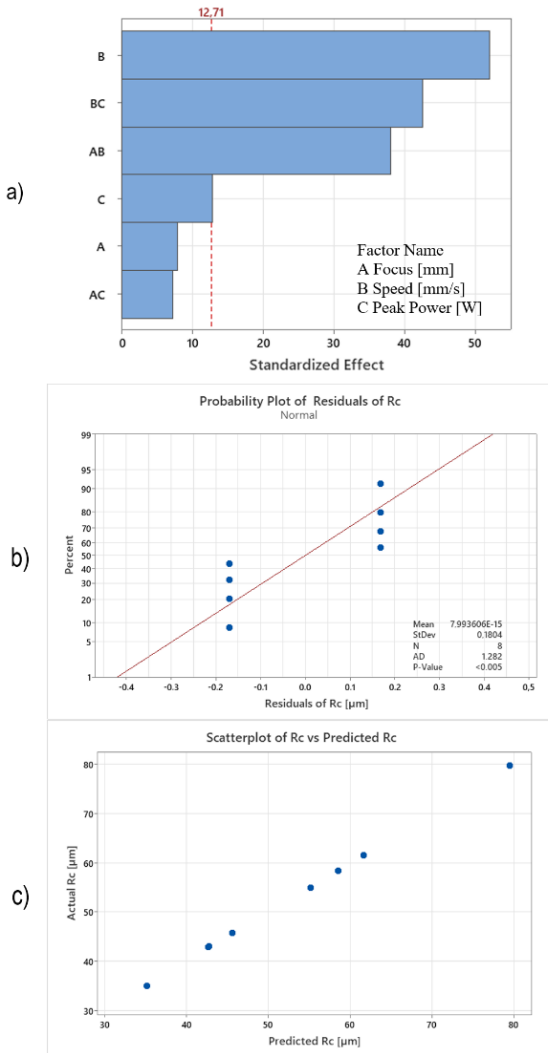


Fig. 5. Pareto chart and diagnostic plots of the EPS production model. (a) Pareto chart of standardized effects, (b) Normal probability plot of residuals, (c) Predicted vs actual values.

In the proposed model, the coefficient of determination (R^2) was relatively high, amounting to 99.98%, and was close to the adjusted coefficient of determination ($R^2 \text{ adj} = 99.89\%$), which confirms the linearity of the regression model. The model's ability to predict new observations was evidenced by the high R^2 values—the predicted value obtained for the reliability of the selected model was 98.97%. The equation of the full regression model, describing the effect of laser setting parameters on roughness, can be expressed as follows:

$$R_c = -3041.0 + 2104.2X_1 + 118.57X_2 + 0.6910 X_3 - 95.26 X_1X_2 + 0.1218 X_1X_3 - 0.026651X_2X_3 \quad (2)$$

A graphical representation of this equation is shown in two-dimensional diagrams in Figure 6.

To ensure low surface roughness in the upper cutting zone under the laser settings presented in Table 1, it is necessary to apply the highest focal length and feed rate, while maintaining the lowest peak power among the analysed cases.

Figure 7 presents example SEM images of the cut surface, obtained using the Axia ChemisSEM Scanning Electron Microscope from ThermoFisher Scientific. The images were taken from the analyzed upper section of the cut surface at magnifications of 200 \times and 2000 \times , providing both macrostructural and microstructural insights into the surface characteristics. Observations were conducted on samples 6 and 8 (see Table 1), which exhibited the highest and lowest R_c roughness values, respectively. The R_c roughness parameter was measured at 79.7 μm for sample 6 and approximately 35 μm for sample 8, indicating a significant difference in surface texture between the two samples.

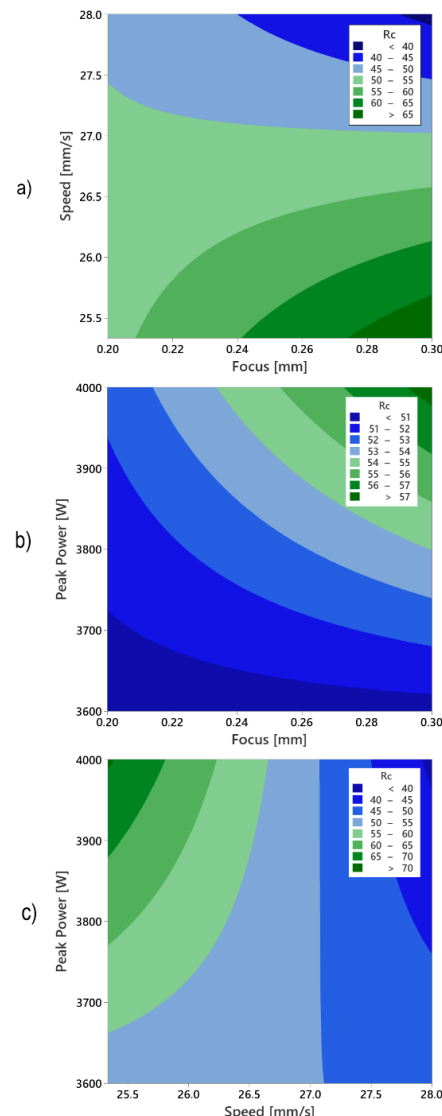


Fig. 6. Influence of control factors on surface roughness R_c : a) Feed and focal speed; (b) Peak and focal power; (c) Peak power and feed speed

It should be noted that striations form on laser-cut surfaces due to the combined effects of laser energy and high-pressure assist gas. These striations are periodic surface patterns that arise from the interaction between the heat generated by the laser and the dynamic forces of the assist gas. In the upper zone of the cut surface, burrs, localized material damage, and microcracks were observed, which may be attributed to thermal stresses during the laser cutting process. These defects, if not controlled, can negatively impact the material's mechanical properties, particularly its fatigue resistance.

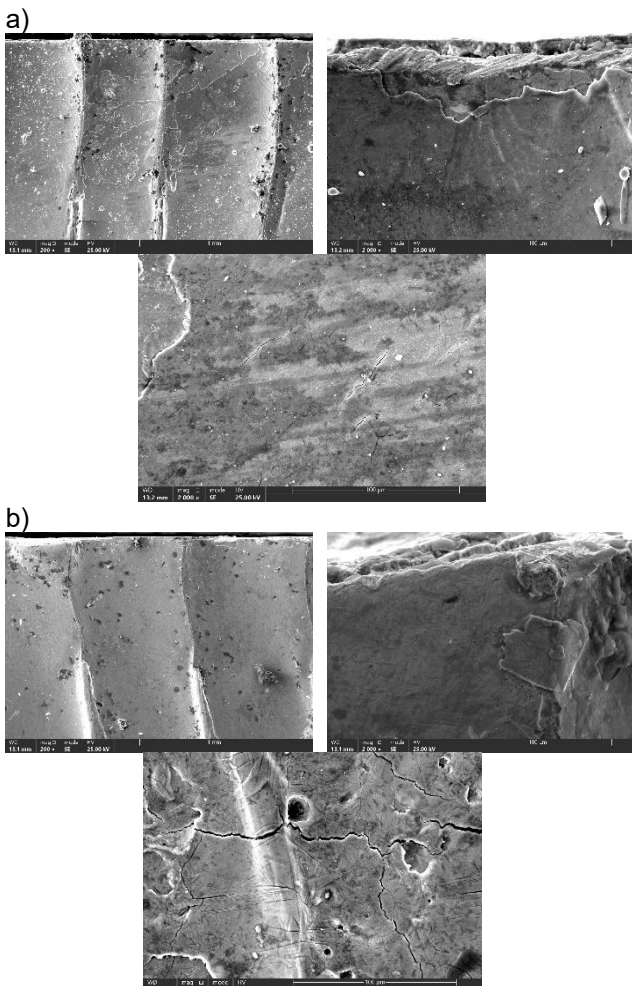


Fig. 7. SEM photographs of the upper part of the cut surface, with visible cracks in the material, a) sample number 8; b) sample number 6 (see table 1)

4. CONCLUSIONS

The following conclusions were drawn from the study:

- Laser-cut edges, produced with the process parameters of focus at 0.3 mm, speed of 28 mm/s, and peak power of 4000W, exhibited the lowest surface roughness, with an R_c value of approximately 35 μm . When the peak power was reduced to 3600W, this parameter increased by approximately 0.3 μm , indicating a correlation between power and surface roughness.
- Optimization via the Response Optimizer (ramp chart, Fig. 8) identified the same parameter combination (focus 0.30 mm, speed 28 mm/s, peak power 4000 W) as optimal for minimizing R_c , with a predicted minimum R_c = 35.24 μm and composite desirability $D=0.996$, consistent with the experimental result.

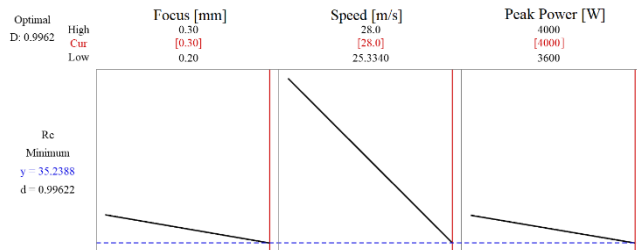


Fig. 8. Response Optimizer ramp chart for R_c : optimal settings focus = 0.30 mm, speed = 28.0 mm/s, peak power = 4000 W; predicted minimum R_c = 35.24 μm with desirability $D=0.996$

- Based on the analysis of the variance of laser cutting parameters for S355J2C+N steel, with respect to the roughness of the upper part of the cut surface (evaluated through the R_c parameter), it was found that the proposed mathematical model describing the influence of the cutting parameters on R_c demonstrated a predicted coefficient of determination of approximately 99.89% ($R^2 \text{ adj} = 99.89\%$). The R_c value is significantly influenced by cutting speed, the interaction of speed and peak power, the interaction of focus and speed, as well as the peak power itself.
- Striation formation on laser-cut surfaces results from the combined effects of laser energy and the high-pressure assist gas used during the cutting process. These striations manifest as periodic surface patterns, which are a direct consequence of the interaction between thermal effects and gas dynamics, leading to variations in material removal efficiency and surface morphology. In the upper zone of the cut surface, further inspection revealed the presence of burrs, localized material damage, and microcracks, likely caused by the thermal stresses and rapid cooling associated with laser cutting. These defects are of particular concern, as they may negatively affect the mechanical properties and fatigue resistance of the processed material. Therefore, the mitigation of these defects is crucial for optimizing laser cutting parameters to ensure better performance and material integrity.

REFERENCES

1. Klimpel A. Theoretical basis of laser cutting of metals. Overview of welding. 2021; 84(6):2-7.
2. Zaborski S, Stechnij T. Thermal methods of shaping from sheets of inox and coal steels. Machine Engineering. 2011;16 (4):109-116.
3. Szulc T. Thermal cutting : perspectives and limitations. Steel. Metals & New Technologies. 2018;3-4:73-77.
4. Klimpel A. Quality of laser cutting of metals. Cutting technologies. Steel. Metafiles & New Technologies. 2012; 48-54.
5. Mazurkiewicz A. Influence of laser cutting parameters on the surface quality. P. 1. Steel. Metals & New Technologies. 2016; 9-10: 112-118.
6. Mazurkiewicz A. Influence of laser cutting parameters on the surface quality. P. 2. Steel. Metals & New Technologies. 2016; 11-12: 25-30.
7. Serei P, Łatka L. Influence of plasma cutting parameters on cut surface quality. Overview of welding. 2016; 8:68-72.
8. Kalashnikov A, Kłos S. Study of the influence of plasma cutting process parameters on product quality. In: Innovations in production management and engineering. Edited by Ryszard Kłosala. Publishing House of the Polish Society for Production Management. Opole. 2018; 1(5): 554-563.

http://46.242.185.119/off_ptzp.org.pl/s107/Artykuly_IZIP_2018

9. Brzozowski A. Quality of surface layer of steel after laser cutting process. In: Scientific Journals of the Poznań University of Technology. Machine Construction and Production Management. 2008; 8:13-20.
10. Kukielka L, Patyk R, Bohdal Ł, Napadlek W, Gryglicki R, Kasprzak P. Investigations of polypropylene foil cutting process using fiber nb: yag and diode nd:YVO₄ lasers. *Acta Mechanica et Automatica*. 2019; 13(2).
11. PN-EN ISO 9013:2017-04: Thermal cutting - Classification of thermal cuts - Geometrical product specification and quality tolerances.
12. Thomas DJ. Finite Element Analysis of Laser Cut Edge Beam Section for High Stress Intensity Structural Assessment. *J Fail. Anal. and Preven.* 2016;16:562–575.
<https://doi.org/10.1007/s11668-016-0124-z>
13. Jakubus, A, Soński MS, Mierzwa P, Stradomski G. Regression Analysis and Optimum Values of Austempering Affecting Mechanical Properties of Compacted Graphite Iron. *Materials*. 2024; 17(20):5024. <https://doi.org/10.3390/ma17205024>
14. Peretz A, Kawačka E, Pude F. Enhancing High-Alloy Steel Cutting with Abrasive Water Injection Jet (AWIJ) Technology: An Approach Using the Response Surface Methodology (RSM). *Materials*. 2024; 17(16):4020. <https://doi.org/10.3390/ma17164020>
15. Fajdek-Bieda A. Optimization of the Geraniol Transformation Process in the Presence of Natural Mineral Diatomite as a Catalyst. *Catalysts*. 2023; 13(4):777. <https://doi.org/10.3390/catal13040777>
16. Perec A, Radomska-Zalas A, Fajdek-Bieda A, Pude F. Process optimization by applying the response surface methodology (RSM) to the abrasive suspension, water, jet cutting of phenolic composites. *Facta Univ. Ser. Moss. Eng.* 2023; 21: 575–589.
17. Ananthakumar K, Rajamani D, Balasubramanian E, Paulo Davim J. Measurement and optimization of multi-response characteristics in plasma arc cutting of Monel 400TM using RSM and TOPSIS. *Measurement* 2019; 135: 725–737.
18. Kheloufi K, El Hachemi A. Numerical investigation of the effect of some parameters on temperature, field and kerf width in laser cutting process. *Phys. Procedia*. 2012; 39: 872–880.
19. Thomas DJ, Whittaker MT, Bright GW, Gao Y. The influence of mechanical and CO₂ laser cut-edge characteristics on the fatigue life performance of high strength automotive steels. *J. Mater. Process. Technol.* 2011; 211: 263–274.
20. PN-EN 10025-2:2007: Hot rolled products of structural steels - Part 2: Technical delivery conditions for non-alloy structured steels - changes in comparison with PN-EN 10025:2002 and their interpretation.
21. Wik B. Study of the influence of laser cutting parameters on the quality of the cut surface of selected materials. Engineering diploma thesis. Supervisor Jasiński M. Jacob of Paradies University. Faculty of Technology. Gorzów Wlkp. Poland 2024.
22. Nowakowski L, Blasiak S, Skrzyniarz M. Influence of the Relative Displacements and the Minimum Chip Thickness on the Surface Texture in Shoulder Milling. *Materials*. 2023;16(24):7661. <https://doi.org/10.3390/ma16247661>
23. Jakubus A. Initial Analysis of the Surface Layer of AVGI Cast Iron Subject to Abrasion. *Archives of Foundry Engineering*. 2022; 22 (2): 1-7.
24. Dyl T, Rydz D, Szarek A, Stradomski G, Fik J, Opydo M. The Influence of Slide Burnishing on the Technological Quality of X2CrNiMo17-12-2 Steel. *Materials*. 2024;17(14):3403. <https://doi.org/10.3390/ma17143403>
25. Wachowicz J, Fik J, Bałaga Z, Stradomski G. Testing for Abrasion Resistance of WC-Co Composites for Blades Used in Wood-Based Material Processing. *Materials*. 2023;16(17):5836. <https://doi.org/10.3390/ma16175836>

Aneta Jakubus:  <https://orcid.org/0000-0003-4940-2919>

Joanna Kostrzewska:  <https://orcid.org/0000-0003-1008-7296>

Marcin Jasiński:  <https://orcid.org/0000-0001-5317-3931>

Bartłomiej Wik:  <https://orcid.org/0009-0008-3873-6263>

Maciej Nadolski:  <https://orcid.org/0000-0001-6099-1369>



This work is licensed under the Creative Commons BY-NC-ND 4.0 license.